



ChemComm

Computational and Experimental Identification of Strong Synergy of Fe/ZnO Catalyst in Promoting Acetic Acid Synthesis from CH₄ and CO₂

Journal:	<i>ChemComm</i>
Manuscript ID	CC-COM-12-2019-010055.R1
Article Type:	Communication

SCHOLARONE™
Manuscripts

COMMUNICATION

Computational and Experimental Identification of Strong Synergy of Fe/ZnO Catalyst in Promoting Acetic Acid Synthesis from CH₄ and CO₂

Received 00th January 20xx,
Accepted 00th January 20xx

DOI: 10.1039/x0xx00000x

Xiaowa Nie,^{*,#,a,b} Xianxuan Ren,^{#,a} Chunyan Tu,^{#,b} Chunshan Song,^{a,c} Xinwen Guo^{*a} and
Jingguang G. Chen^{*b}

DFT calculations have identified reaction pathways for acetic acid synthesis from CO₂ and CH₄ on ZnO, Cu/ZnO and Fe/ZnO surfaces. Fe/ZnO exhibits strong synergy in facilitating CH₄ activation, dissociation and the C-C coupling. Thus the surface acetate formation is significantly enhanced. The DFT predictions have been confirmed by in situ DRIFTS experiments.

Production of valuable chemicals from CO₂ and CH₄, attracts great attention due to their potential utilization as alternative feedstocks while mitigating greenhouse gases, which represents a promising approach in green chemistry and CO₂ utilization.¹ Transformation of CO₂ with CH₄ to value-added products is one of the ideal approaches combining an oxidation and a reduction reaction, however, this process is scientifically and technically challenging, due to the chemical inertness of the two molecules. Acetic acid synthesis is one of the promising reactions in direct transformation of CO₂ with CH₄, and attracts great interest due to the high market value of acetic acid as an important raw material in organic chemical industry.² This method has 100% atomic efficiency, however, is thermodynamically unfavorable due to the large positive Gibbs free energy change ($\Delta G^0 = 16.98$ kcal/mol). The equilibrium amount of acetic acid formation from conversion of CO₂ and CH₄ are calculated at different conditions (see **Figure S1**), which illustrates the dependence on reaction temperature and pressure. Significant efforts have been put into the development of effective catalysts, including homogeneous (e.g. Pd(OAc)₂/Cu(OAc)₂/O₂/CF₃COOH³), heterogeneous (e.g. metal-exchanged zeolite^{4, 5}) and photocatalysts,⁶ as well as utilizing catalytic dielectric-barrier discharge.⁷ Metal oxides and metal-

modified zeolites are commonly used as heterogeneous catalysts for the conversion of CO₂ and CH₄.^{4,5} However, most of the systems require high temperature to activate and convert both CO₂ and CH₄, and the selectivity and yield of acetic acid are still low (e.g. yield of 395 μ mole gcat⁻¹ h⁻¹ at 773 K⁴). Solid-state NMR spectroscopy has been used to study the mechanism of transformation of CO₂ with CH₄ to acetic acid over Zn-modified HZSM-5 at relatively high temperatures (523 to 773 K).⁸ CH₄ activation and dissociation occur at the Zn sites to form a Zn-CH₃* intermediate, the Zn-C bond of which then goes through the insertion by CO₂ to generate surface acetate species. Acetic acid formation is accomplished by proton transfer from the Brønsted acid site of HZSM-5 to adsorbed acetate. A recent theoretical study by Zhang *et al.* has reported that the catalytic activity of CO₂ and CH₄ conversion to acetic acid strongly depends on the local structure of active sites of Zn-modified H-ZSM-5 zeolite.⁵ On Zn-doped ceria catalyst, facile CH₄ activation and C-C coupling are revealed by Ge *et al.* using density functional theory (DFT) calculations.⁹ An Eley-Rideal (E-R) mechanism is proposed for surface acetate formation, in which gas phase CO₂ inserts into the σ -bond of Zn-CH₃*. However, the final step of acetic acid formation from acetate hydrogenation is highly endothermic (1.3 eV), limiting the rate for the overall conversion. Their follow-up work reported a concurrent activation of CH₄ and CO₂ at the zinc oxide-indium oxide interface in acetic acid synthesis.¹⁰ The reaction mechanism is altered due to CO₂ adsorption on the defective In₂O₃ surface before insertion into Zn-CH₃*, following a typical Langmuir-Hinshelwood (L-H) mechanism. Although the (ZnO)₃/In₂O₃(110) surface is catalytically more active toward acetic acid formation than Ga₂O₃/In₂O₃(110) and (ZrO₂)₃/In₂O₃(110), both the CH₄ dissociation and CO₂ insertion steps have larger barriers on the mixed oxide surfaces than those obtained over Zn/CeO₂(111) in the previous study.⁹

These studies demonstrate that zinc and zinc oxide are important components for CH₄ activation, however, it is still challenging to simultaneously promote the three key elementary steps (CH₄ activation, C-C coupling, and H addition) involved in acetic acid formation. Design of active and robust catalysts for acetic acid synthesis directly from CO₂ and CH₄ remains scientifically and practically limited. Fe-based catalysts are active for hydrocarbons

^a State Key Laboratory of Fine Chemicals, PSU-DUT Joint Center for Energy Research, School of Chemical Engineering, Dalian University of Technology, Dalian, Liaoning 116024, P.R. China. E-mail: niexiaowa@dlut.edu.cn; guoxw@dlut.edu.cn

^b Department of Chemical Engineering, Columbia University, New York, NY 10027, USA. E-mail: jgchen@columbia.edu

^c EMS Energy Institute, PSU-DUT Joint Center for Energy Research, Department of Energy & Mineral Engineering, Pennsylvania State University, University Park, PA 16802, USA.

These authors contributed equally to this work.

Electronic Supplementary Information (ESI) available: [details of any supplementary information available should be included here]. See DOI: 10.1039/x0xx00000x

and alcohols synthesis via promoting C-C coupling and carbon chain growth.¹¹ Meanwhile, they are also active for CH₄-involved reactions such as conversion to syngas.¹² Therefore, it is of great interest to investigate the role of Fe in direct transformation of CO₂ with CH₄ to acetic acid, which would be potentially promising when combining with zinc oxide since these two components both show good activities in CO₂ or CH₄ related reactions.¹⁰⁻¹² Herein, we present results of the mechanisms of acetic acid synthesis from CO₂ and CH₄ over the Fe/ZnO catalyst by combining DFT calculations and in situ DRIFTS experiments. Parallel studies are conducted on pure ZnO and Cu/ZnO for comparison. For the first time, a strong synergy of the Fe/ZnO catalyst in promoting the acetic acid synthesis from CH₄ and CO₂ is identified, on which the barriers for CH₄ dissociation and C-C coupling are significantly lower as compared to those on ZnO and Cu/ZnO. The side reactions such as CO₂ hydrogenation as well as CH₃* decomposition can be effectively suppressed on Fe/ZnO, leading to an enhanced production of surface acetate species. DFT results are confirmed by in situ DRIFTS experiments on surface species identification.

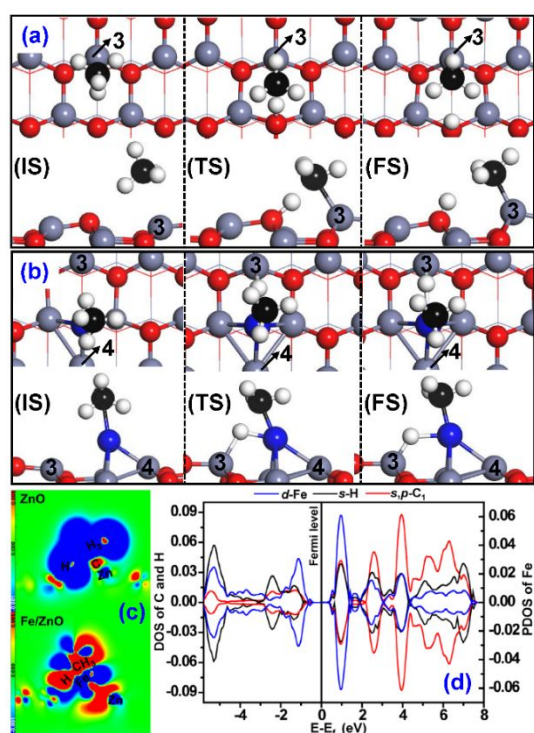


Figure 1. Optimized structures of initial, transition and final states associated with CH₄ dissociation on (a) ZnO(10 $\bar{1}$ 0) and (b) Fe/ZnO(10 $\bar{1}$ 0) surfaces (grey: Zn, blue: Fe, red: O, black: C, white: H). (c) Electron density difference maps of transition states for CH₄ dissociation on the two surfaces. (d) DOS and PDOS of transition state for CH₄ dissociation on Fe/ZnO(10 $\bar{1}$ 0).

On ZnO(10 $\bar{1}$ 0), CH₄ adsorption on the Zn site is weak, with a binding energy of -0.06 eV calculated by the PBE functional and with a dispersion correction of -0.32 eV. CH₄* dissociation proceeds through breaking one of the C-H bonds at the Zn site, with the dissociated H atom bonding to an adjacent surface O site (**Figure 1a**). The dissociation barrier is 0.93 eV, close to the value (0.97 eV) reported by Shavi *et al.*¹³ The CO₂ molecule is adsorbed at the Zn-O-

Zn site with a binding energy of -0.83 eV. Subsequent C-C coupling occurs via the insertion of CO₂* into the σ -bond of Zn-CH₃*, leading to the formation of a bidentate acetate (η^2 -CH₃COO*) species bound to two surface Zn atoms (**Figure S3a**). The C-C coupling barrier is 1.46 eV and exothermic by 0.73 eV. Therefore, ZnO itself is not active for acetic acid synthesis due to a high C-C coupling barrier and slow CH₄ activation.

When Fe is doped onto the ZnO(10 $\bar{1}$ 0) surface by taking up an O vacancy site, the modified surface electronic properties and structures can induce the alteration of reaction pathways and kinetics, thereby affecting the selectivity and yield of acetic acid. CH₄ adsorption is stronger on the Fe site of Fe/ZnO, with a binding energy of -0.37 eV calculated by PBE and -0.58 eV with dispersion corrections included. The dissociation of CH₄ occurs through breaking one of the C-H bonds at the Fe site, with the dissociated H atom bonding to an adjacent Zn₃ site (**Figure 1b**). In the transition state, the H_{diss} atom coordinates to both the Fe and Zn₃ sites, with the H_{diss}-Fe and H_{diss}-Zn₃ distances being 1.70 and 1.84 Å, respectively. The C-H_{diss} bond is lengthened to 1.76 Å, indicating larger activation degree than the transition state generated on ZnO, which has a C-H_{diss} distance of 1.48 Å. The dissociation barrier is significantly reduced on Fe/ZnO, which is only 0.30 eV, much lower than that (0.93 eV) obtained on pure ZnO. Electronic features are analyzed to explore the observed difference on CH₄ activation/dissociation between ZnO and Fe/ZnO. Bader charge results show that the pure ZnO surface transfers 0.064|e| to CH₄ molecule comparing the transition to the adsorbed state, whereas for Fe/ZnO, Fe metal and ZnO transfer 0.27|e| and 0.081|e| to CH₄, respectively, rendering CH₄ activation more pronounced in the dissociation process. The electron density difference maps (**Figure 1c**) illustrate that on pure ZnO, main electron transfer occurs from the ZnO surface to the C atom of CH₃* species but the surface-adsorbate interaction is not strong due to the small electron density accumulation on the CH₃*-H* state. On Fe/ZnO, substantial electron transfer from Fe to CH₃*-H* is observed and the surface-adsorbate interaction is much stronger, making the transition state more stable. These electronic properties are consistent with the trend in the activation barriers, demonstrating an enhanced activity of Fe/ZnO toward CH₄ activation/dissociation. In addition, the density of states (DOS) and projected DOS (PDOS) of the transition state associated with CH₄ dissociation on Fe/ZnO(10 $\bar{1}$ 0) are calculated and shown in **Figure 1d**. Significant overlaps between the *s*, *p* orbitals of C and *d* states of Fe are observed, as well as between the *s* orbital of H_{diss} and *d* states of Fe. These observations indicate strong interactions between Fe and the CH₃*-H* species, leading to the formation of Fe-C and Fe-H_{diss} bonds in the transition state of CH₄ dissociation.

Subsequent C-C coupling proceeds with Fe-CH₃* and a co-adsorbed CO₂ at an adjacent Zn-O-Zn site, following a L-H mechanism for CO₂ insertion (**Figure S3b**), with a C-C coupling barrier of 0.84 eV. However, the H_{diss} adsorbed at the original dissociated Zn₃-Fe site has a steric effect on C-C coupling. An alternative pathway is also examined, wherein the H_{diss} first migrates to a Zn₄-Fe bridge site on the other side of Zn₃-CH₃* (**Figure S4**), which only has a barrier of 0.23 eV. With this new H_{diss} location, the C-C coupling barrier reduces to 0.75 eV. Therefore, both the location and the adsorption stability of H_{diss} have an impact on C-C coupling kinetics over Fe/ZnO. The facile C-C coupling on Fe/ZnO renders it a good candidate for

acetic acid synthesis. This C-C coupling barrier is lower than that calculated by Shavi *et al.* on other single oxide catalyst such as CeO₂(111) (2.83 eV)¹³ as well as those obtained by Zhao *et al.* on mixed (ZnO)₃/In₂O₃(110) (1.45 eV) and Ga₂O₃/In₂O₃ (2.04 eV) surfaces.¹⁰ Electronic features are further analyzed to explain the reduced barrier on Fe/ZnO compared to pure ZnO. The CO₂ molecule acquires 0.749 |e| and 0.980 |e| during the formation of C-C coupling transition states on ZnO and Fe/ZnO, respectively, and the transition states on the two surfaces are 0.520 |e| and 0.717 |e| negatively charged, respectively. These results are indicative of stronger interactions of CO₂* with both the CH₃* species and the Fe/ZnO surface, enhancing the stability of the transition state. The electron density difference maps (Figure S3c) demonstrate that on Fe/ZnO, substantial electron accumulation is achieved around the C atom of CH₃*, O atom of CO₂* as well as the H_{diss}, while electrons are depleted around the C atom of CO₂* and surface Fe, indicating strong electronic interactions in CO₂*-CH₃*, Fe-CO₂*, Fe-CH₃* and Fe-H*. Thus, enhanced stability of the transition state for C-C coupling can be achieved on Fe/ZnO, leading to the reduced kinetic barrier. The DOS and PDOS of the C-C coupling transition state (Figure S3d) illustrate substantial overlaps between the *s*, *p* orbitals of C₂ in CO₂* and *s*, *p* orbitals of C₁ in CH₃*, showing the tendency of C-C bond formation in the transition state. Overlaps between *d* states of Fe and *s*, *p* orbitals of C₁ in CH₃* indicate that the binding interaction of Fe-CH₃* still plays a role in transition state formation, consistent with the transition state configuration shown in Figure S3b. CO₂* interacts with both the Zn₁ and Fe sites and orbital overlaps of *s* orbital of Zn with *s*, *p* orbitals of O₁ in CO₂* and *d* states of Fe with *s*, *p* orbitals of C₂ in CO₂* are observed. These results demonstrate strong bimetallic synergy of Fe-Zn in promoting the C-C coupling between Fe-CH₃* and CO₂*.

The C-C coupling leads to the formation of an adsorbed bidentate acetate (η^2 -CH₃COO*) species. On pure ZnO, the η^2 -CH₃COO* is bound to the surface Zn₁ and Zn₃ sites and the direct hydrogenation of O₂ with H_{diss} produces the acetic acid product. This H addition step has a small barrier of 0.32 eV with the reaction being endothermic by 0.27 eV. Acetic acid desorption should be kinetically slow, with a desorption energy of 1.09 eV. On Fe/ZnO, the η^2 -CH₃COO* species binds to the Zn₁ and Fe sites. CH₃COO* hydrogenation with the H_{diss} adsorbed at the Zn₄-Fe bridge site needs to overcome a large barrier (1.95 eV) and a strong endothermic reaction energy (1.85 eV). Instead, another H_{diss} migration step is explored before acetic acid formation on Fe/ZnO, in which the H_{diss} migrates to a surface O₃ site prior to acetate hydrogenation (Figure S4). Although the migration barrier (0.99 eV) is not small, it is more favorable than the direct hydrogenation of acetate. More importantly, with this new H_{diss} location, the acetic acid formation becomes more facile, with a reaction energy of only 0.2 eV and zero barrier. It is worth noting that the produced CH₃COOH* is a metastable state on both ZnO and Fe/ZnO, in which the H_{diss} atom also strongly interacts with the surface O₃ site while binding to O₁ of CH₃COOH* (Figure S5). Although the final desorption of acetic acid from the surface is slow, formation of the surface acetate species is dramatically more favorable on the Fe/ZnO surface, due to the fast CH₄ activation/dissociation, facile C-C coupling, and easy H addition.

In the synthesis of acetic acid over heterogeneous catalysts, several by-products are detected in experiments such as formic acid and methanol.² Here the formation of the primary by-product formic acid (HCOOH) is examined over Fe/ZnO(10 $\bar{1}$ 0), which can be produced from CO₂* hydrogenation via a COOH* or HCOO* intermediate (Figure S6). The barriers are 1.64 and 1.43 eV for COOH* and HCOO* formation, respectively, indicating that the production of formic acid by-product is not facile on Fe/ZnO. In addition, the dissociation of CH₃* to CH₂*+H* has a barrier of 1.19 eV, kinetically unfavorable than the C-C coupling of CH₃* with CO₂* (0.75 eV). These DFT results reveal that the side reactions are significantly suppressed on Fe/ZnO (Figure S7), leading to an enhanced selectivity to the desired acetic acid product.

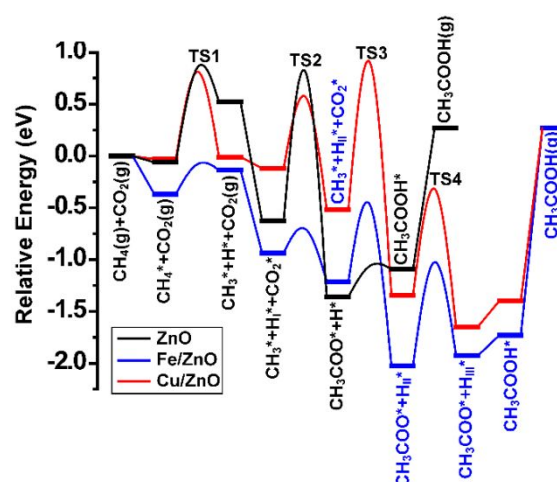


Figure 2. Energy profiles of acetic acid synthesis from CO₂ and CH₄ on ZnO(10 $\bar{1}$ 0), Cu/ZnO(10 $\bar{1}$ 0) and Fe/ZnO(10 $\bar{1}$ 0) surfaces (H₁* denotes the initial H_{diss} site from CH₄ dissociation, H₁₁* represents the first H_{diss} migration from the initial Zn₃-M to Zn₄-M bridge site, and H₁₁₁* stands for the second H_{diss} migration from the Zn₄-M bridge site to surface O₃ site on Cu/ZnO and Fe/ZnO).

To shed light on whether other 3d transition metal doped ZnO has comparable activity to Fe/ZnO, similar calculations are performed on Cu/ZnO. DFT results are provided in the **Supporting Information**. The pathways for acetic acid formation on Cu/ZnO are similar to Fe/ZnO, but its catalytic activity should be much lower than Fe/ZnO, as illustrated in Figure 2. Especially, CH₄ dissociation and C-C coupling have larger barriers on Cu/ZnO, making the formation of surface acetate species more difficult. However, formate formation from CO₂ hydrogenation is facile, with a barrier of 1.12 eV. Therefore, formate would be the dominant surface species during CO₂ reaction with CH₄ on Cu/ZnO.

In situ DRIFTS experiments have been conducted to identify the surface species formation during CH₄+CO₂ reaction and after purging reactants over ZnO, Cu/ZnO and Fe/ZnO (Figure 3). Two strong bands at 1500~1520 cm⁻¹ and 1320~1340 cm⁻¹ are assigned to monodentate carbonates.^{14, 15} Under reaction conditions, only monodentate carbonates (1508 and 1332 cm⁻¹) and some hydrogen carbonates (1607 and 1375 cm⁻¹)¹⁵ are formed on the surface of ZnO support, indicating that ZnO itself is not active for converting CO₂+CH₄. The monodentate carbonates are also observed on Cu/ZnO and Fe/ZnO, which are originated from CO₂ adsorption over the O

sites. Typical stretching vibrational modes of formate at 1592 and 1369 cm^{-1} are observed on Cu/ZnO and Fe/ZnO.^{15, 16} However, Cu/ZnO exhibits stronger feature of formate species, indicating that formate is the dominant surface species during converting CO_2 and CH_4 (consistent with DFT results). When removing the reactants of CO_2 and CH_4 from the DRIFTS cell, the vibrational modes of formate species become weaker gradually and diminishes after 30 min. Interestingly, unlike ZnO and Cu/ZnO, the Fe/ZnO catalyst shows the O=C=O stretching modes at 1538 and 1448 cm^{-1} under reaction conditions of CO_2+CH_4 mixture, which are assigned to the surface bidentate acetates ($\eta^2\text{-CH}_3\text{COO}^*$).^{16, 17} These species completely disappear after purging reactants for 10 min, suggesting that the bidentate acetate formed on Fe/ZnO is an active surface intermediate. In order to further identify the formation of surface bidentate acetate on Fe/ZnO, a “ CH_4 off- CH_4 on” experiment is performed to observe the dynamic change of surface species over Fe/ZnO (Figure S12). No bands at around 1538 and 1448 cm^{-1} are observed during the adsorption of CO_2 alone for 30 min. However, when CH_4 is introduced into the CO_2 gas stream, peaks at 1538 and 1448 cm^{-1} appear and become more intense after 30 min. These two new bands are attributed to surface bidentate acetate formed on Fe/ZnO, which are identical to those species formed by the adsorption of acetic acid.^{16,17} These peaks become invisible gradually after cutting off of CH_4 and CO_2 , confirming that the active surface acetate is formed in the presence of both CH_4 and CO_2 on Fe/ZnO under the reaction condition. The detection of monodentate carbonates on ZnO, Cu/ZnO and Fe/ZnO identified by DRIFTS is also consistent with DFT calculations (See Figures S3 and S8). Therefore, the DFT-predicted synergy of Fe/ZnO in facilitating acetate formation is supported by the in situ DRIFTS experiments.

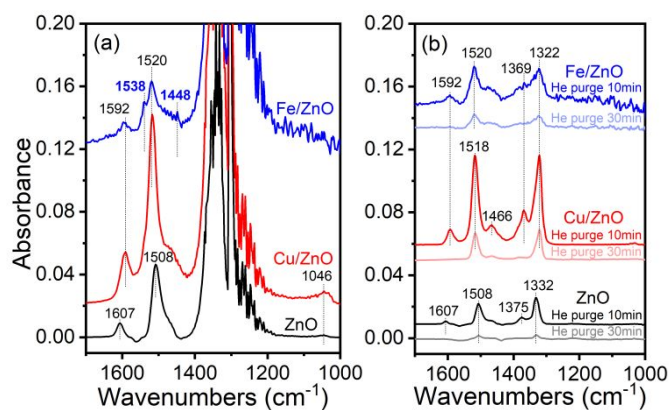


Figure 3. In situ DRIFTS spectra of (a) CH_4+CO_2 reaction and (b) spectra after He purge over ZnO, Cu/ZnO and Fe/ZnO at 673 K.

In conclusion, DFT calculations reveal reaction pathways for acetic acid synthesis from CO_2 and CH_4 on ZnO, Cu/ZnO and Fe/ZnO surfaces. ZnO itself is not active due to large barriers for CH_4 activation and C-C coupling. Cu/ZnO is catalytically inactive either, due to large barriers for CH_4 dissociation, C-C coupling and surface H^* migration, while formate is the dominant surface species in the conversion of CO_2 and CH_4 on this surface. Doping ZnO with Fe leads to a strong synergy in promoting acetic acid formation, with both CH_4 activation/dissociation and C-C coupling being facilitated.

Consequently, the formation of surface acetate is significantly enhanced. DFT results on comparing the pathways and activities of the three catalysts are verified by the in situ DRIFTS experiments. This work provides insight into the understanding of mechanisms for acetic acid synthesis from CO_2 and CH_4 , and paves an avenue for designing efficient transition metal doped ZnO catalysts for future studies.

This work is supported by the National Key Research and Development Program of China under Contract No. 2016YFB0600902. C.T. and J.G.C. acknowledge support by the U.S. Department of Energy (DOE), Catalysis Science Program, under Contract No. DE-SC0012704. We acknowledge Dr. Zhenhua Xie for performing calculations of thermodynamic equilibrium concentrations.

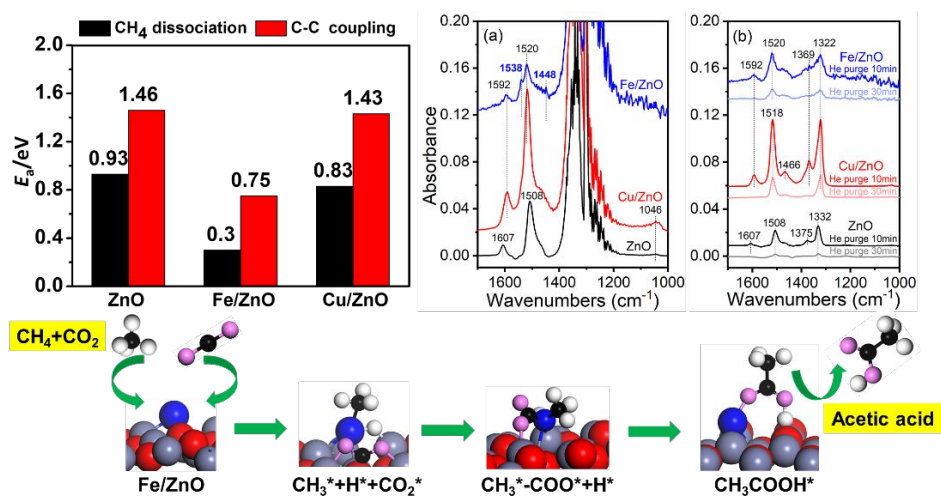
Conflicts of interest

There are no conflicts to declare.

References

- 1 C. Song, *Catal. Today*, 2006, **115**, 2-32.
- 2 W. Huang, K. C. Xie, J. P. Wang, Z. H. Gao, L. H. Yin and Q. M. Zhu, *J. Catal.*, 2001, **201**, 100-104.
- 3 K. Masanobu, N. Kazuyuki, J. Tetsuro, T. Yuki, T. Ken and F. Yujo, *Chem. Lett.*, 1995, **24**, 244-244.
- 4 A. M. Rabie, M. A. Betiha and S.-E. Park, *Appl. Catal. B: Environ.*, 2017, **215**, 50-59.
- 5 P. Zhang, X. Yang, X. Hou, J. Mi, Z. Yuan, J. Huang and C. Stampfl, *Catal. Sci. Technol.*, 2019, **9**, 6297-6307.
- 6 N. Yazdanpour and S. Sharifnia, *Sol. Energ. Mat. Sol. C.*, 2013, **118**, 1-8.
- 7 C. J. Liu, L. Yang, Y. P. Zhang, Y. Wang, J. J. Zou, E. Baldur and B. Z. Xue, *Chem. Lett.*, 2001, **30**, 1304-1305.
- 8 J.-F. Wu, S.-M. Yu, W. D. Wang, Y.-X. Fan, S. Bai, C.-W. Zhang, Q. Gao, J. Huang and W. Wang, *J. Am. Chem. Soc.*, 2013, **135**, 13567-13573.
- 9 Y. Zhao, C. Cui, J. Han, H. Wang, X. Zhu and Q. Ge, *J. Am. Chem. Soc.*, 2016, **138**, 10191-10198.
- 10 Y. Zhao, H. Wang, J. Han, X. Zhu, D. Mei and Q. Ge, *ACS Catal.*, 2019, **9**, 3187-3197.
- 11 H. Yang, C. Zhang, P. Gao, H. Wang, X. Li, L. Zhong, W. Wei and Y. Sun, *Catal. Sci. Technol.*, 2017, **7**, 4580-4598.
- 12 N. Deshpande, A. Majumder, L. Qin and L. S. Fan, *Energ. Fuel.*, 2015, **29**, 1469-1478.
- 13 R. Shavi, J. Ko, A. Cho, J. W. Han and J. G. Seo, *Appl. Catal. B Environ.*, 2018, **229**, 237-248.
- 14 A. M. Turek, I. E. Wachs and E. DeCanio, *J. Phys. Chem.*, 1992, **96**, 5000-5007.
- 15 G. N. Vayssilov, M. Mihaylov, P. S. Petkov, K. I. Hadjiivanov and K. M. Neyman, *J. Phys. Chem. C*, 2011, **115**, 23435-23454.
- 16 V. Matsouka, M. Konsolakis, R. M. Lambert and I. V. Yentekakis, *Appl. Catal. B-Environ.*, 2008, **84**, 715-722.
- 17 W. Rachmady and M. A. Vannice, *J. Catal.*, 2002, **207**, 317-330.

Graphical abstract



A combined DFT and DRIFTS study identified the synergy of Fe/ZnO in promoting acetic acid synthesis from CO₂ and CH₄